

See discussions, stats, and author profiles for this publication at: <https://www.researchgate.net/publication/7746419>

# Probing Intramolecular Förster Resonance Energy Transfer in a Naphthaleneimide–Peryleneimide–Terrylenediimide–Based Dendrimer by Ensemble and Single-Molecule Fluorescence Spectrosc...

ARTICLE in JOURNAL OF THE AMERICAN CHEMICAL SOCIETY · AUGUST 2005

Impact Factor: 12.11 · DOI: 10.1021/ja042656o · Source: PubMed

CITATIONS

115

READS

12

7 AUTHORS, INCLUDING:



Tom Vosch

University of Copenhagen

100 PUBLICATIONS 3,804 CITATIONS

SEE PROFILE



Satoshi Habuchi

King Abdullah University of Science and Tech...

71 PUBLICATIONS 2,167 CITATIONS

SEE PROFILE



Johan Hofkens Prof

University of Leuven

398 PUBLICATIONS 11,271 CITATIONS

SEE PROFILE



Frans C De Schryver

University of Leuven

670 PUBLICATIONS 21,225 CITATIONS

SEE PROFILE

## Probing Intramolecular Förster Resonance Energy Transfer in a Naphthaleneimide–Peryleneimide–Terrylenediimide-Based Dendrimer by Ensemble and Single-Molecule Fluorescence Spectroscopy

Mircea Cotlet,<sup>†,‡</sup> Tom Vosch,<sup>†</sup> Satoshi Habuchi,<sup>†,||</sup> Tanja Weil,<sup>§</sup> Klaus Müllen,<sup>§</sup> Johan Hofkens,<sup>\*,†,⊥</sup> and Frans De Schryver<sup>\*,†</sup>

Contribution from the Department of Chemistry, Katholieke Universiteit Leuven, Celestijnenlaan 200 F, Heverlee B-3001, Belgium, Bioscience Division, Los Alamos National Laboratory, Mail Stop J586, Los Alamos, New Mexico 87545, Max-Planck-Institut für Polymerforschung, Ackermannweg 10, 55128 Mainz, Germany, and Unité CMAT, Université Catholique de Louvain, Bâtiment Lavoisier Place L. Pasteur 1, 1348 Louvain-la-Neuve, Belgium

Received December 7, 2004; E-mail: johan.hofkens@chem.kuleuven.ac.be; frans.deschryver@chem.kuleuven.ac.be

**Abstract:** We report on the ensemble and single-molecule (SM) dynamics of Förster resonance energy transfer (FRET) in a multichromophoric rigid polyphenylenic dendrimer (triad) with spectrally different rylene chromophores featuring distinct absorption and emission spectra which cover the whole visible spectral range: a terrylenediimide (TDI) core, four perylenemonoimides (PMIs) attached at the scaffold, and eight naphthalenemonoimides (NMIs) at the rim. For FRET from PMI to TDI taking place with an efficiency of 99.5%, single triad molecules optically excited at 490 nm show fluorescence exclusively from the TDI side in the beginning of their emission. On 360-nm excitation, NMI chromophores transfer their excitation energy either directly or in a stepwise fashion to the core TDI, the latter case involving scaffold-substituted PMIs as intermediate acceptors. Indeed, SM experiments on 360-nm excitation evidence highly efficient FRET from NMI chromophores to the TDI core since individual triad molecules show fluorescence exclusively either from TDI or from an intermediate (oxidized) species but never from PMI. Because PMI and TDI are chromophores with high fluorescence quantum yields and high resistance to photobleaching compared to NMI, 360-nm excitation of a single triad molecule leads to bleaching of NMI chromophores with no chance for PMI to be observed. The spatial positioning and the spectral properties of the chosen rylene chromophores make this multichromophoric system an efficient light collector, able to capture light over the whole visible spectral range and to transfer it finally to the core TDI, the latter releasing it as red fluorescence.

### Introduction

Light-harvesting systems of plants and bacteria are designed to capture, transport, and finally convert visible light into a chemically usable form of energy. The transport of light to the reaction center involves absorption of light and unidirectional transfer of the absorbed radiation energy by many chromophores with adequate spectral properties and relative position/orientation toward each other. Transfer of the absorbed radiation energy to the reaction center spans a distance of several nanometers and is achieved by a multistep Förster resonance energy-transfer (FRET) mechanism.<sup>1</sup> Artificial systems capable of multistep unidirectional energy transfer have been the subject of intense research.<sup>2–4</sup> In such systems with several chromophores absorb-

ing light in different regions of the visible spectral range, unidirectional energy transfer takes place from the chromophore with the energetically highest  $S_0$ – $S_1$  transition to the chromophore with the energetically lowest  $S_0$ – $S_1$  transition. The

- (1) (a) McDermott, G.; Prince, S. M.; Freer, A. A.; Hawthornthwaite-Lawless, A. M.; Papiz, M. Z.; Cogdell, R. J.; Isaacs, N. W. *Nature* **1995**, *374*, 517–521. (b) Kühlbrandt, W.; Wang, D. N. *Nature* **1991**, *350*, 130–134. (c) Kühlbrandt, W.; Wang, D. N.; Fujiyoshi, Y.; *Nature* **1994**, *367*, 614–621. (d) Kühlbrandt, W. *Nature* **1995**, *374*, 497–498. (e) Glazer, A. N. *Annu. Rev. Biophys. Chem.* **1985**, *14*, 47–77. (f) Adronov, A.; Gilat, S. L.; Fréchet, J. M. J.; Ohta, K.; Neuwahl F. V. R.; Fleming, G. R. *J. Am. Chem. Soc.* **2000**, *122*, 1175–1185.
- (2) (a) Webber, S. E. *Chem. Rev.* **1990**, *90*, 1469–1482. Fox, M. A. *Acc. Chem. Res.* **1992**, *25*, 569–574. (b) Watkins, D. M.; Fox, M. A. *J. Am. Chem. Soc.* **1994**, *116*, 6441–6442. (c) Gust, D.; Moore, T. A.; Moore, A. L. *Acc. Chem. Res.* **1993**, *26*, 198–205. (d) Gust, D.; Moore, T. A.; Moore, A. L. *Acc. Chem. Res.* **2001**, *34*, 40–48. Heilemann, M.; Tinnefeld, P.; Mosteiro, G. S.; Parajo, M. G.; Van Hulst, N. F.; Sauer, M. *J. Am. Chem. Soc.* **2004**, *126*, 6514–6515. (e) Hausteint, E.; Jahnz, M.; Schwill, P. *ChemPhysChem* **2003**, *4*, 745–748. (f) Hohng, S.; Joo, C.; Ha, T. *Biophys. J.* **2004**, *87*, 1328–1337. (g) Shortreed, M. R.; Swallen, S. F.; Shi, Z.-Y.; Tan, W.; Xu, Z.; Devadoss, C.; Moore, J. S.; Kopelman, R. *J. Phys. Chem. B* **1997**, *101*, 6318–6322. (h) Hahn, U.; Gorka, M.; Vogtle, F.; Vicinelli, V.; Ceroni, P.; Maestri, M.; Balzani, V. *Angew. Chem.* **2002**, *41*, 3595–3598.
- (3) Weil, T.; Reuter, E.; Müllen, K. *Angew. Chem., Int. Ed.* **2002**, *41*, 1900–1904.

<sup>†</sup> Katholieke Universiteit Leuven.

<sup>‡</sup> Los Alamos National Laboratory.

<sup>§</sup> Max-Planck-Institut für Polymerforschung.

<sup>⊥</sup> Université Catholique de Louvain.

<sup>||</sup> Present address: Department of Biological Chemistry and Molecular Pharmacology, Harvard Medical School, 240 Longwood Ave., SGM 209, Boston, MA 02115.

process may involve a chromophore intermediate in terms of  $S_0$ – $S_1$  energetics. However, if the emission spectrum of the chromophore with the energetically highest  $S_0$ – $S_1$  transition overlaps with a  $S_0$ – $S_n$  absorption band of the chromophore with the energetically lowest  $S_0$ – $S_1$  transition, and if both chromophores are at favorable distance and orientation for FRET, the intermediate chromophore might be bypassed in terms of transfer of energy. If so, competition between direct and cascade energy transfer may occur.<sup>4</sup> Here we investigate competition between direct and cascade FRET in a rigid polyphenylene dendrimer containing three structurally and spectrally distinct types of rylene chromophores. Dendrimers are macromolecules with a perfectly controllable branched structure consisting of three structural units—the core, a hyperbranched shell, and an external surface—individual layers around the core being designated as generations. Fluorescent chromophores can be attached either to the external surface of the dendrimer or as a core. Thus, dendrimer synthesis serves as a way to obtain a well-defined number of chromophores in a confined volume element. Not only can the number of chromophores be controlled, but also the interactions among them can be governed by changing the structure of the branches to which they are attached or by attaching the branches to different cores. Using such an approach, researchers have probed interactions of the dendritic branches, conformational distortions, and intramolecular excitation energy transfer or electron transfer among chromophores.<sup>5–11</sup> If decorated with photostable chromophores such as rylene dyes, dendrimers can be addressed in single-molecule fluorescence studies, thus allowing photophysical processes to be probed at the most detailed level.<sup>7–12</sup>

For the multichromophoric system studied here, the design comprises a third-generation globular polyphenylene dendrimer (Figure 1a, triad) that bears a terrylenediimide (TDI) chromophore as a core (Figure 1a, TDI), perylenemonoimide (PMI) chromophores in the scaffold (Figure 1a, PMI), and naphthalenemonoimide (NMI) chromophores at the rim (Figure 1a, NMI). With spectrally different chromophores positioned at the periphery, in the scaffold, and in the core, the triad absorbs light over the whole visible range of the spectrum and emits mainly in the red region of the visible spectrum due to FRET involving different types of rylene chromophores. The polyphenylene arms confer rigidity to the system, thus avoiding conformational flexibility, the latter greatly influencing FRET efficiency parameters.<sup>3</sup>

## Material and Methods

Details of the synthesis of the triad (Figure 1a) are given elsewhere.<sup>3</sup> Figure 1a contains also structures of model compounds carrying single NMI, PMI, and TDI moieties, respectively.

**Ensemble Spectroscopy.** Stationary spectroscopic experiments were performed on a Perkin-Elmer Lambda 40 spectrophotometer (absorption) and a Spex Fluorolog 1500 fluorimeter (Spex Industries, Metuchen, NJ; fluorescence). Fluorescence quantum yields were estimated by using either cresyl violet in ethanol or anthracene in cyclohexane as a reference (quantum yields of 0.51 and 0.38, respectively). Fluorescence decays were recorded by the time-correlated single-photon-counting (TCSPC) technique.<sup>13</sup> In brief, linearly polarized laser excitation at either 360 or 490 nm was provided by a frequency-doubled/mode-locked picosecond Ti:sapphire laser (Tsunami Spectra Physics; 1.2-ps pulse, 8.13-MHz repetition rate); 640-nm pulsed excitation was achieved by using a diode laser (PDL 800, Picoquant GmbH). Fluorescence was collected at the magic angle (54.7°), spectrally separated by a monochromator (Sciencetech 9030, 10-nm bandwidth), and detected with a microchannel plate photomultiplier (MCP-PMT, Hamamatsu E 3059-500). The electronic signal from the MCP-PMT was sent into a TCSPC card (SPC 630, Becker-Hickl GmbH). Fluorescence decays were collected in 4096 channels and were analyzed by iterative reconvolution.<sup>5</sup> The contribution of the decay times were estimated as relative amplitudes according to  $a_j^{\text{rel}} = a_j/\sum a_j$ .

**Single-Molecule Detection.** Samples for single-molecule experiments were prepared by spin-casting, either on a glass (490-nm and longer excitation) or on a quartz (360-nm excitation) coverslip, a droplet of a toluene solution of the dendrimer ( $10^{-10}$  M concentration) mixed with polymer (Zeonex). Room-temperature single-molecule fluorescence experiments were performed on a scanning stage confocal epimicroscope coupled to the picosecond laser system used for ensemble TCSPC (vide supra). Optical excitation with either 360- or 490-nm pulsed laser light occurred through an oil immersion objective lens (Olympus 1.4 NA, 60×). For 490-nm excitation, the collected fluorescence was filtered from the excitation light by using a dichroic mirror (DRLP500 Chroma Technologies) and a notch filter (490 nm, Kaiser Optics). Using an 80%/20% beam-splitter cube, part of the collected fluorescence (20%) was spectrally resolved into a polychromator (Acton 150, Acton Research) attached to a back-illuminated cooled charged-coupled device camera (LNCCD, Roper Scientific), and the rest (80%) was spectrally separated by a second dichroic mirror (DRPL650 Chroma Technologies) into green and red colors, with each of the colors confocally imaged onto single-photon-counting avalanche photodiodes (APDs) (SPCM 15 EG&G). Cross-talking between APDs was avoided by inserting additional filters in the detection path (HQLP690 and HQSP620, Omega Filters, for the red and the green APD, respectively). For 360-nm excitation, we used a similar two-color detection scheme, except for the 80%/20% beam-splitter cube. Single-molecule fluorescence trajectories were registered by the TCSPC PC card operated in FIFO (first-in, first-out) mode. In this mode, single-molecule trajectories are registered such that for each detected photon the time lags with respect to the excitation pulse (microtime) and with respect to the previously detected photon (chronological time) are stored. Such information allows construction of two-color fluorescence intensity trajectories and decay histograms of certain bin and amount of photons (here 1000), respectively.<sup>14–16</sup>

- (4) Serin, J. M.; Brousmiche, D. W.; Fréchet, J. M. J. *Chem. Commun.* **2002**, 22, 2605–2607.
- (5) De Backer, S.; Prinzie, Y.; Verheijen, W.; Smet, M.; Desmedt, K.; Dehaen, W.; De Schryver, F. C. J. *Phys. Chem. A* **1998**, 102, 5451–5455.
- (6) Pollak, K. W.; Leon, J. W.; Frechet, J. M. J.; Maskus, M.; Abruna, H. D. *Chem. Mater.* **1998**, 10, 30–38.
- (7) Hofkens, J.; Maus, M.; Gensch, T.; Vosch, T.; Cotlet, M.; Köhn, F.; Herrmann, A.; Müllen, K.; De Schryver, F. C. J. *Am. Chem. Soc.* **2000**, 122, 9278–9288.
- (8) Gronheid, R.; Stefan, A.; Cotlet, M.; Hofkens, J.; Van der Auweraer, M.; Verhoeven, J. W.; Müllen, K.; De Schryver, F. C. *Angew. Chem., Int. Ed.* **2003**, 42, 4209–4214.
- (9) Cotlet, M.; Gronheid, R.; Habuchi, S.; Stefan, A.; Barbafiga, A.; Müllen, K.; Hofkens, J.; De Schryver, F. C. J. *Am. Chem. Soc.* **2003**, 125, 13609–13617.
- (10) Gronheid, R.; Hofkens, J.; Köhn, F.; Weil, T.; Reuther, E.; Müllen, K.; De Schryver, F. C. J. *Am. Chem. Soc.* **2002**, 124, 2418–2419.
- (11) Cotlet, M.; Masuo, S.; Luo, G.; Hofkens, J.; Van der Auweraer, M.; Verhoeven, J.; Müllen, K.; Xie, X. S.; De Schryver, F. C. *Proc. Natl. Acad. Sci. U.S.A.* **2004**, 101, 14343–14348.
- (12) Métivier, R.; Kulzer, F.; Weil, T.; Müllen, K.; Basché, T. *J. Am. Chem. Soc.* **2004**, 126, 14364–14365.

- (13) Maus, M.; Rousseau, E.; Cotlet, M.; Schweitzer, G.; Hofkens, J.; Van der Auweraer, M.; De Schryver, F. C.; Krueger, A. *Rev. Sci. Instrum.* **2001**, 72, 36–41.
- (14) Cotlet, M.; Hofkens, J.; Habuchi, S.; Dirix, G.; Van Guise, M.; Michiels, J.; Vanderleyden, J.; De Schryver, F. C. *Proc. Natl. Acad. Sci. U.S.A.* **2001**, 98, 14398–1443.
- (15) Maus, M.; Cotlet, M.; Hofkens, J.; Gensch, T.; De Schryver, F. C.; Schaffer, J.; Seidel, C. A. M. *Anal. Chem.* **2001**, 73, 2078–2086.
- (16) Eggeling, C.; Fries, J. R.; Gunther, R.; Seidel, C. A. M. *Proc. Natl. Acad. Sci. U.S.A.* **1998**, 95, 1556–1561.

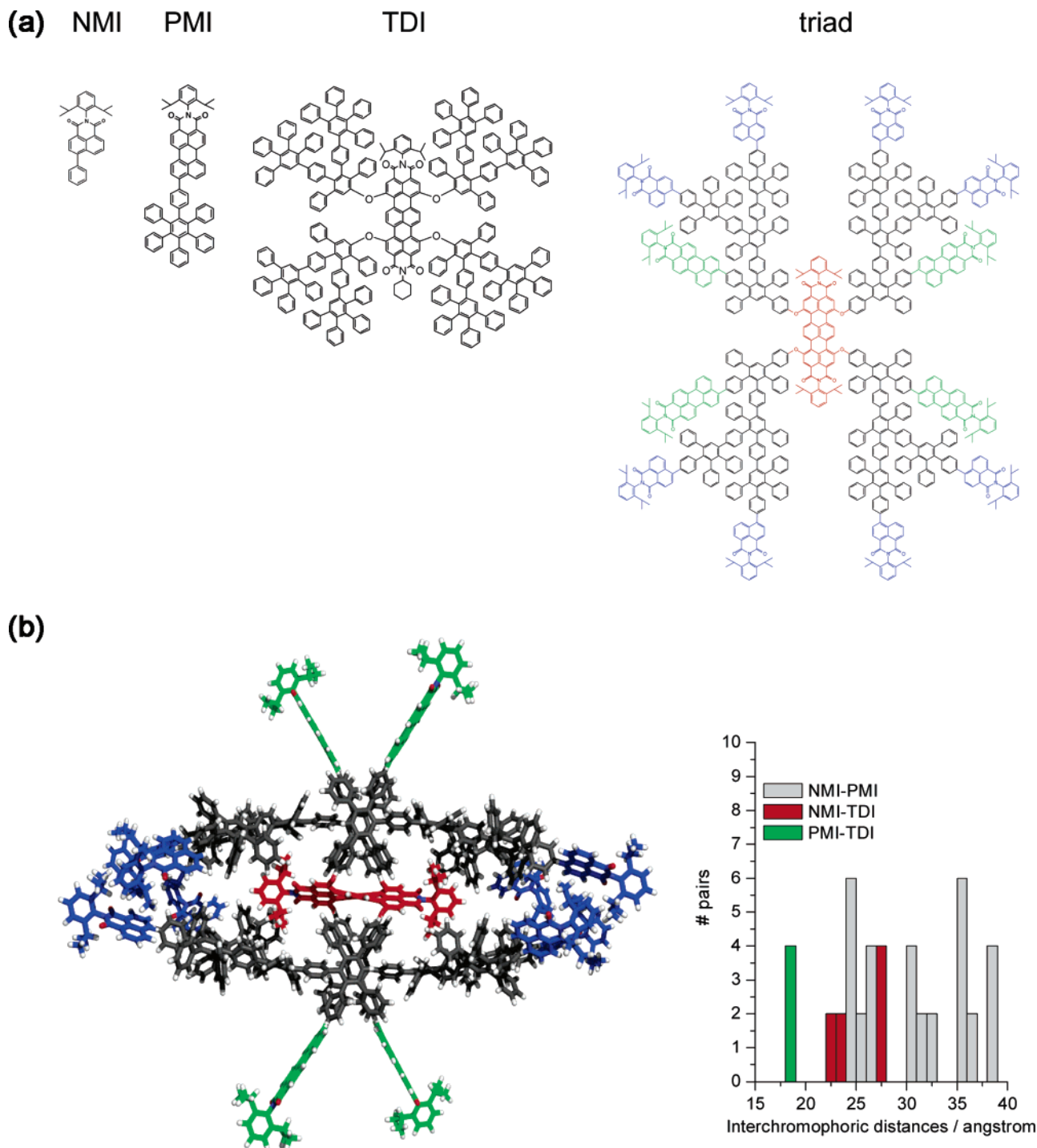


**Figure 1.** (a) Structures of the model compounds containing naphthalenemonoimide (NMI), perylenemonoimide (PMI), and terrylenediimide (TDI) moieties, respectively, and of the triad. For the triad, NMI, PMI, and TDI chromophores are colored in blue, green, and red, respectively. (b) Left side: energetically minimized structure of the triad. Right side: NMI–PMI (gray), NMI–TDI (red), and PMI–TDI (green) center-to-center distances estimated from the energetically minimized structure.

## Results and Discussion

**Ensemble Spectroscopy.** Shown in Figure 2a are the absorption and the fluorescence spectra of the triad in toluene ( $10^{-6}$  M). The absorption and the fluorescence spectra of the model compounds in toluene ( $\sim 10^{-6}$  M) are depicted in Figure 2b. Model NMI absorbs maximally at around 350 nm with an extinction coefficient of about  $21\,000\text{ M}^{-1}\text{ cm}^{-1}$  and fluoresces maximally at around 420 nm with a quantum yield of  $\sim 0.1$ . Fluorescence from the model NMI (360-nm excitation, 420-

nm detection) decays single exponentially with a lifetime of 0.33 ns (Table 1). For model PMI, the visible region of the absorption spectrum in toluene features two peaks at 496 and 522-nm, with an extinction coefficient at 522 nm of  $38\,300\text{ M}^{-1}\text{ cm}^{-1}$  (Figure 2b). In the ultraviolet region, model PMI absorbs maximally at around 350 nm, a peak assigned to the  $S_0$ – $S_2$  absorption of the PMI chromophore. Model PMI fluoresces maximally at around 560 nm (Figure 2b, 490-nm excitation), with a quantum yield of fluorescence in toluene of 0.98 and a



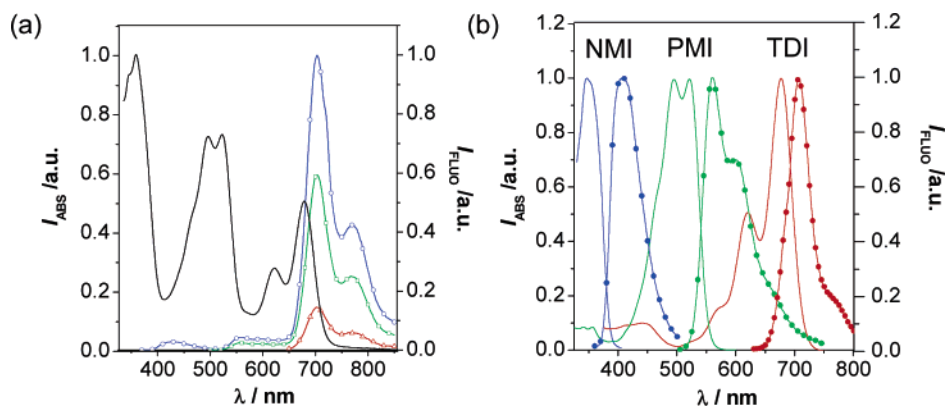


**Figure 2.** (a) Absorption (black line) and fluorescence (line + symbol) spectra of the triad in toluene. Fluorescence spectra were recorded upon excitation at 360 nm (blue), 490 nm (green), or 640 nm (red). (b) Absorption (line) and fluorescence (line + symbol) spectra in toluene of the model compounds containing NMI (blue graphs, 360-nm excitation), PMI (green graphs, 490-nm excitation), and TDI (red graphs, 640-nm excitation) moieties, respectively.

**Table 1.** Time-Correlated Single-Photon-Counting Results for the Model Compounds and Triad in Toluene<sup>a</sup>

	Excitation:	360 nm			490 nm		640 nm
	Detection:	420 nm	560 nm	705 nm	560 nm	705 nm	705 nm
NMI		0.33 (100%)			4.3 (100%)		
PMI							
TDI							3.2 (92%), 0.95 (5%), 0.12 (3%)
triad		0.33 (3%), 0.04 (96%)	4 (13%), 0.03 (87%)	3.2 (47%), 0.95 (5%), 0.04 (48%)	4 (6%), 0.02 (94%)	3.2 (68%), 0.95 (5%), 0.02 (27%)	

<sup>a</sup> Values for fluorescence decay times are given in nanoseconds and their respective contributions are shown in parentheses. Values for the triad shown in italics have negative contribution.

fluorescence lifetime of 4 ns (Table 1). Model TDI absorbs maximally at 677 nm, with an extinction coefficient of  $85\,500\text{ M}^{-1}\text{ cm}^{-1}$ , and it shows an additional peak at 440 nm related to the  $S_0$ – $S_2$  absorption (Figure 2b).<sup>17</sup> Fluorescence from the model TDI (640-nm excitation) peaks around 670 nm (Figure 2b); it has a quantum yield of 0.99 in toluene and decays multiexponentially (Table 1). We have shown previously that the multiexponential decay of fluorescence from TDI reflects a distribution of ground-state conformers of the TDI chromophore caused by the torsion induced by the dendritic sidearms attached to the bare chromophore.<sup>17</sup>

The triad absorbs over the whole visible spectral range with distinct peaks at 358, 522, and 677 nm related to the substituted NMI, PMI, and TDI chromophores, respectively (Figure 2a). These peaks are well separated, thus making optical excitation of distinct rylene chromophores within the triad possible. Independent of the excitation wavelength, the triad fluoresces with a main peak at 706 nm, i.e., fluorescence from the core TDI (Figure 2a). On 490-nm excitation, the fluorescence spectrum of the triad shows an additional band peaking at 560 nm, related to the PMI chromophores (Figure 2b). On 360-nm excitation, the fluorescence spectrum of the triad shows two additional bands peaking at 430 and 560 nm (Figure 2a), related to the rim-substituted NMIs and the scaffold-substituted PMIs, respectively.

Table 1 contains time-correlated single-photon-counting (TCSPC) results for the triad on 360- and 490-nm excitation, respectively. On 490-nm excitation, the fluorescence decay

detected at the emission peak of PMI (560 nm) is best fitted with a biexponential model with decay times of 0.02 ns (94% contribution) and 4 ns (6%), and the fluorescence decay detected at the emission peak of TDI (705-nm) is best fitted with a three-exponential model including two rise times of 0.02 ns (27% contribution) and 0.95 ns (5%) and a decay time of 3.2 ns (68%). On 360-nm excitation, the fluorescence decay detected at the emission peak of NMI is best fitted with a biexponential model with decay times of 0.04 ns (96% contribution) and 0.33 ns (3%), the fluorescence decay detected at the emission peak of PMI is best fitted with a biexponential model with decay times of 0.03 (87% contribution) and 4 ns (13%), and the fluorescence decay detected at the emission peak of TDI is best fitted with two rise times of 0.04 ns (48% contribution) and 0.95 ns (5%) and a decay time of 3.2 ns (47%). Figure 1b is the energetically optimized 3D structure of the triad by using the Merck Molecular Force Field (molecular mechanics method) embedded in Spartan 5. Based on this structure, the center-to-center distances between different types of rylene chromophores are 1.85 nm between PMI and TDI, from 2.45 to 3.85 nm between NMI and PMI, and from 2.25 to 2.75 nm between NMI and TDI (graph in Figure 1). PMI emission and TDI absorption overlap considerably, and the same observation is true for NMI emission and PMI absorption (Figure 2a). Therefore, conditions are fulfilled in terms of distance and spectral overlap for unidirectional FRET from the scaffold-substituted PMIs to the core TDI and from the rim-substituted NMIs to PMIs. On the basis of the spectral data of the model compounds and of the triad, we find Förster radii of 5.9 and 3 nm for unidirectional FRET from PMI to TDI and from NMI to PMI, respectively.<sup>18</sup> Therefore, on 490-nm excitation of the triad, PMI fluorescence

(17) Schweitzer, G.; Gronheid, R.; Jordens, S.; Lor, M.; De Belder, G.; Weil, T.; Reuther, E.; Müllen, K.; De Schryver, F. C. *J. Phys. Chem. A* **2003**, *107*, 3199–3207.

is strongly quenched due to unidirectional FRET to the core TDI. FRET from PMI to TDI is detected here as a decay time of 0.02 ns at the emission peak of PMI and as a rise time at the emission peak of TDI. A reduction in the lifetime of PMI from 4 ns (the case of model PMI) to 0.02 ns (the case of triad) reflects an efficiency of FRET from PMI to TDI of 99.5%. For a Förster radius for energy transfer of 5.9 nm<sup>18</sup> and an interchromophoric distance of 1.85 nm for the PMI–TDI chromophore pair, the efficiency of FRET from PMI to TDI is 91%, in agreement with the experimental value from the 490-nm excitation TCSPC experiments. The 4-ns decay time detected at 540 nm and with a small contribution relates to unquenched PMI fluorescence, probably due to either decoupled PMI chromophores or triad molecules having an optically inactive TDI core.<sup>17</sup>

Strong quenching is experienced also by the fluorescence emitted by the rim-substituted NMIs on 360-nm excitation of triad. Here we detect a reduction in the lifetime of NMI from 0.33 ns (Table 1, the case of model NMI) to 0.04 ns (Table 1, 360-nm excitation, 430-nm detection, the case of triad). On the basis of the spectral overlap between NMI emission and PMI absorption, we estimate a Förster radius for energy transfer for the NMI–PMI chromophore pair of 3 nm.<sup>18</sup> For an interchromophoric NMI–PMI distance of 2.45–3.85 nm, quenching of NMI fluorescence is suggested to be the result of energy transfer from NMI to PMI. However, NMI fluorescence overlaps also with the S<sub>0</sub>–S<sub>2</sub> absorption band of TDI (Figure 2a), and molecular geometry optimization indicates NMI and TDI chromophores can reach an interchromophoric distance as short as 2.25 nm. On the basis of the spectral overlap between the NMI fluorescence and TDI S<sub>0</sub>–S<sub>2</sub> absorption bands, we estimate a Förster radius for the NMI–TDI FRET of 2.6 nm.<sup>18</sup> Thus, unidirectional FRET from rim-substituted NMIs to the core TDI is not to be excluded and will therefore compete with unidirectional FRET to scaffold-substituted PMIs. Consequently, on 360-nm excitation of the triad, the excitation energy from an NMI chromophore can be transferred to the core TDI either directly or in a cascade fashion, the latter case with the participation of a PMI chromophore as intermediate acceptor for NMI and intermediate donor for TDI. Giving the possibility of an NMI-to-TDI unidirectional FRET occurring on 360-nm excitation of the triad and competing with the NMI-to-PMI transfer, we can now understand why, within the time resolution of the TCSPC experiments, the fluorescence detected at the emission peak of PMI lacks a rise time component related to the NMI–PMI transfer. With time constants as fast as a few tens of picoseconds and relatively close in values, a rise time in the decay detected upon 360-nm excitation of the triad at the emission peak of PMI, reflecting the NMI-to-PMI transfer, will be canceled by the decay time reflecting the PMI-to-TDI transfer. We find experimental evidence for unidirectional NMI–TDI transfer here through the perfect match in value

between the decay time detected in the 430-nm fluorescence decay (emission peak of NMI) and the rise time detected in the 705-nm fluorescence decay (emission peak of TDI).

Ensemble spectroscopic data reported here in connection with the triad clearly demonstrate that unidirectional FRET takes place between NMI–PMI, NMI–TDI, and PMI–TDI chromophore pairs, respectively, and transfer of excitation energy from NMI to TDI may or may not involve a PMI chromophore as an intermediate. However, in ensemble-averaged experiments, dynamic information is usually smeared out, and eventual heterogeneity is difficult if not impossible to detect. This is because such data are averaged over a large number of molecules and hide differentiated behavior at the molecular level. Such hidden information can be extracted by single-molecule spectroscopy. Here, we use multidimensional single-molecule fluorescence detection (MSMD), a method allowing simultaneously acquisition, from each individual molecule, of time trajectories of several molecular properties (vide infra). Introduced by Keller and co-workers and refined by Seidel and co-workers, MSMD was proven to successfully allow identification of different emitting species in both synthetic and biological multichromophoric systems and to follow FRET dynamics in biological molecules/complexes.<sup>7,14,16,19,20</sup>

**Single-Molecule Detection on 490-nm Excitation.** Shown in Figures 3 and 4 are results obtained from single triad molecules immobilized in Zeonex under ambient conditions and excited with 490-nm pulsed laser light. They refer to MSMD experiments where we record simultaneously the fluorescence intensity and the fluorescence lifetime from the core TDI (TDI channel) and/or from the scaffold-substituted PMIs (PMI channel), the fractional intensity, and the fluorescence spectrum. Fractional intensity is defined as  $F(t) = I_{\text{TDI}}(t)/(I_{\text{TDI}}(t) + I_{\text{PMI}}(t))$ , with  $I_{\text{TDI}}(t)$  and  $I_{\text{PMI}}(t)$  the fluorescence intensities in the TDI and PMI channels, respectively.  $F(t)$  is a property we can use to judge the activity in the TDI and PMI channels and therefore the efficiency of FRET from PMI to TDI.

According to the ensemble FRET data we report here, highly efficient FRET is expected to occur when probing single triad molecules with 490-nm laser light. Indeed, at this excitation wavelength and for an average power at the sample of 0.8 kW/cm<sup>2</sup>, we detect fluorescence from single molecules of the triad mainly in the TDI channel, i.e., emission from the core TDI (vide infra).

Within 100 triad molecules we have probed with 490-nm excitation, a large subpopulation of molecules (83%) shows exclusive activity in the TDI channel, before complete photobleaching occurs (Figure 3a, upper and lower panels). For such molecules,  $F(t)$  shows a constant value around unity (Figure 3a), therefore proving a highly efficient FRET occurs from the scaffold-substituted PMIs to the TDI core. Following the trajectory of the fluorescence lifetime and of the fluorescence spectrum of these molecules, both parameters stay constant during the survival time, suggesting emission is related to a single excited species, here the TDI chromophore.<sup>9,10</sup> The fluorescence intensity in the TDI channel decreases in a stepwise fashion because of successive photobleaching of the PMI donors

(18) The values for  $R_0$  were calculated using  $R_0 = 0.211[\kappa^2 n^{-4} Q_D J(\lambda)]^{1/6}$  (Å) by assuming an orientation factor  $\kappa$  of 0.667, a refractive index of 1.4969, and a quantum yield of fluorescence of the donor  $Q_D$  of 0.98 for PMI and 0.1 for NMI. The overlap integrals  $J(\lambda)$ , expressed here in M<sup>-1</sup> cm<sup>-1</sup> (nm)<sup>4</sup>, were calculated on the basis of the spectral data reported in the main text for both the triad and the model compounds and were found to be  $5.85 \times 10^{14}$  for NMI–PMI,  $2.39 \times 10^{14}$  for NMI–TDI, and  $3.78 \times 10^{15}$  for PMI–TDI.  $J(\lambda)$  for NMI–TDI originates from the overlap between the S<sub>0</sub>–S<sub>2</sub> absorption of TDI and the fluorescence of NMI. In view of the fact that a mixture of isomers results from the synthesis, this approach was chosen rather than a more detailed calculation, such as that reported in, e.g.: Scholes, G. D. *Annu. Rev. Phys. Chem.* **2003**, *54*, 57–87.

(19) Rothwell, P. J.; Berger, S.; Kensch, O.; Felekyan, S.; Antonik, M.; Wohrl, B. M.; Restle, T.; Goody, R. S.; Seidel, C. A. M. *Proc. Natl. Acad. Sci. U.S.A.* **2003**, *100*, 1655–1660.

(20) Shera, E. B.; Seitzinger, N. K.; Davis, L. M.; Keller, R. A.; Soper, S. A. *Chem. Phys. Lett.* **1990**, *174*, 553–557.

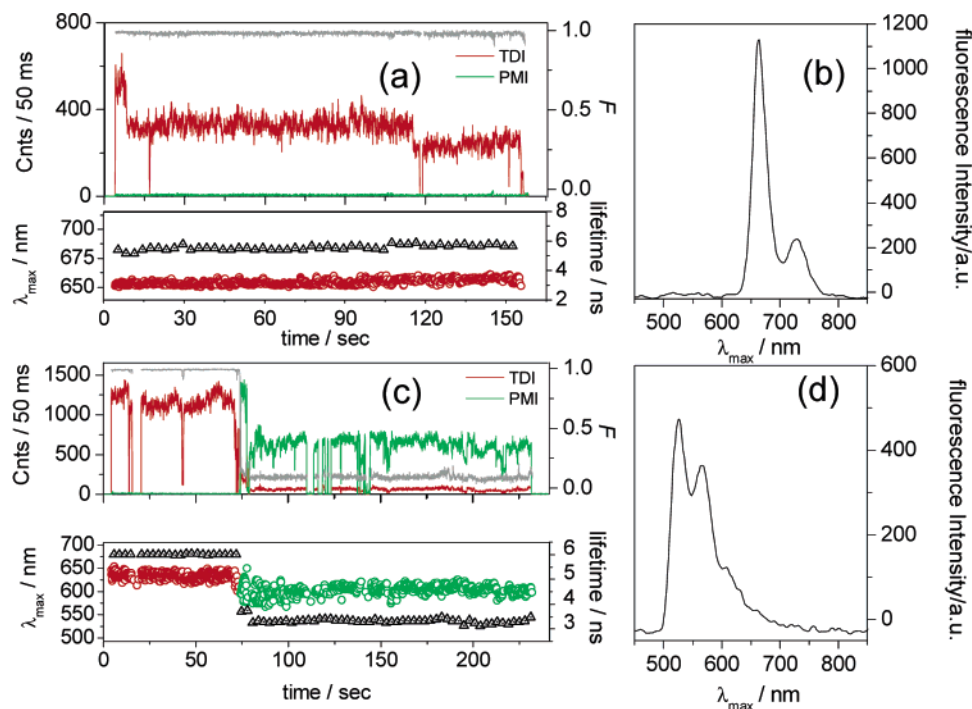


**Figure 3.** Single-molecule results on 490-nm excitation of triad in Zeonex. Properties estimated with photons detected in the TDI channel are colored red, and those estimated with photons from the PMI channel are green. (a) Upper panel: trajectories of the fluorescence intensity (red and green lines) and fractional intensity (gray line) from a single triad molecule. Lower panel: trajectories of the fluorescence lifetime (red circles) and emission maximum (black triangles) from the single triad molecule accounting for the upper panel. (b) Fluorescence spectrum (3-s integration time) detected from the single molecule accounting for panel a. (c) Upper panel: trajectories of the fluorescence intensity (red and green lines) and fractional intensity (gray line) from a single triad molecule. Lower panel: trajectories of the fluorescence lifetime (red and green circles) and emission maximum (black triangles) from the single triad molecule accounting for the upper panel. (d) Fluorescence spectrum (3-s integration time) detected from the single molecule accounting for panel c after the bleaching of TDI.

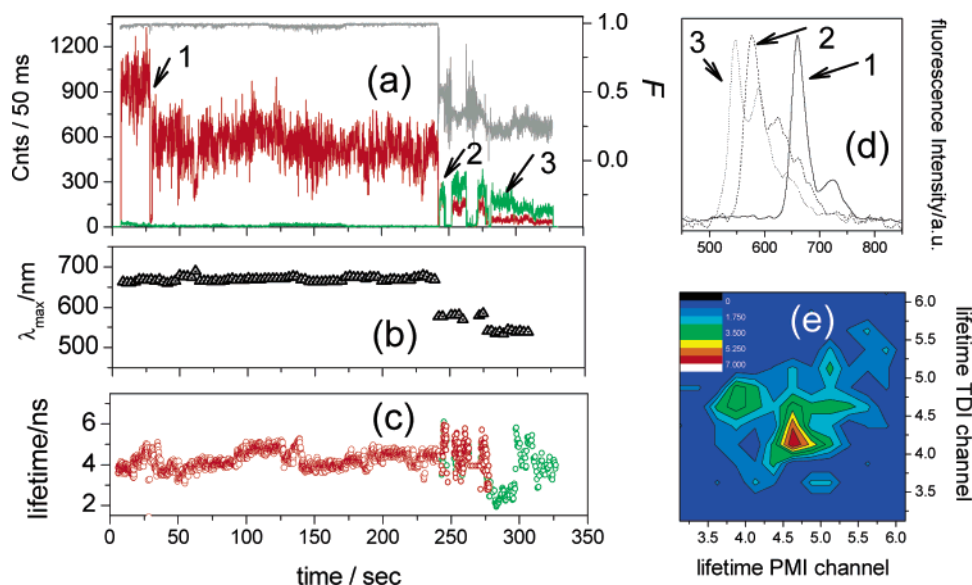


**Figure 4.** Single-molecule results on 490-nm excitation of a triad molecule embedded in Zeonex. Properties estimated with photons detected in the TDI channel are colored red, and those estimated with photons from the PMI channel are green. (a) Trajectories of the fluorescence intensity (red and green lines) and of the fractional intensity (gray line). (b) Trajectory of the emission maximum (black triangles). (c) Trajectories of the fluorescence lifetimes detected in the TDI (red circles) and PMI (green circles) channels. (d) Fluorescence spectra (3-s integration time) detected in the regions indicated in panel a and related to TDI emission (spectrum 1), emission from an intermediate species (spectrum 2), and PMI emission (spectrum 3). (e) Contour plot showing the correlation between lifetimes detected in the TDI and PMI channels in the region from 250 to 270 s shown in panel a, upper side.

(Figure 3a, upper panel).<sup>9,10</sup> Fluorescence spectra detected from such molecules peak around 680 nm (Figure 3b) and resemble, both in shape and in peak position, the ensemble solution spectrum of the model TDI (Figure 2b).<sup>9,17</sup> Fluorescence lifetimes detected in the TDI channel show values ranging from 3 ns (lifetime of the bare TDI) up to 9 ns, similar to those we

observed previously for single diad molecules immobilized in Zeonex, i.e., dendrimers based on a TDI core and four rim-substituted PMIs.<sup>9</sup> For the diad, a broad distribution of single-molecule lifetimes detected from the TDI core was connected with the presence of a distribution of ground-state TDI conformers as a result of the torsion induced by the dendritic arms



attached to the core chromophore; therefore, similar reasoning can be invoked for the triad.

The second subpopulation of triad molecules (17%) shows emission in the PMI channel only after the bleaching of the TDI core (Figure 3c, upper and lower panels). Bleaching of TDI is followed by the appearance of a single-molecule (SM) fluorescence spectrum peaking around 540 nm (Figure 3d) and resembling in shape the ensemble solution spectrum of PMI (Figure 2a). Such a SM spectrum is detected always together with SM fluorescence lifetimes of around 4 ns, a value characteristic for PMI.<sup>9,17</sup> Here, bleaching of the TDI followed by emission from PMI is seen as a change in the value of  $F(t)$  from 1 to nearly 0 (Figure 3c, upper panel) and therefore as a change in FRET efficiency from 100% to zero because of the disappearance (photobleaching) of the acceptor chromophore.

Figure 4 is an example of a single triad molecule where bleaching of the TDI core is not followed by the emission from PMI(s) but from an intermediate species with a fluorescence spectrum peaking around 590 nm (Figure 4d, spectrum 2). For this individual molecule, bleaching of TDI (Figure 4a–c at around 240 s) is accompanied by a hypsochromic shift in the SM fluorescence spectrum from 670 nm to 590 nm (Figure 4b) and a drop in the fractional intensity  $F(t)$  from 1 to 0.5 (Figure 4a). A value of 0.5 for  $F(t)$  accounts for equal contributions of the fluorescence signal in both TDI and PMI channels. It is interesting to note the shape resemblance between the SM spectrum of TDI (Figure 4d, spectrum 1 peaking at 670 nm) and the SM spectrum of the intermediate species (Figure 4d, spectrum 2 peaking at 590 nm). Moreover, the SM lifetimes we detect in the TDI and PMI channels and simultaneously with the SM spectrum peaking at 590 nm are correlated (Figure 4e), suggesting that the emission is related to a single species, i.e., the intermediate one. After bleaching of the intermediate, we detect fluorescence mainly in the PMI channel (Figure 4a–c with  $F(t) \approx 0.2$ ) and a SM fluorescence spectrum characteristic of PMI (Figure 4d, spectrum 3 peaking at 540 nm). We have seen such an intermediate in 5% of the population of individual triad molecules interrogated at 490-nm excitation. The resemblance in shape between the SM spectra of TDI and those of the intermediate makes us believe the latter species is an oxidized TDI chromophore with a reduced extent of conjugation and therefore with spectrally blue-shifted absorption and emission properties compared to TDI.<sup>21</sup> Being immobilized, individual triad molecules can undergo many optical excitation cycles. If so, the emitting chromophore, here TDI, has the chance to eventually visit the triplet state, even if it has a low intersystem crossing yield (as suggested by its high quantum yield of fluorescence), and therefore to react with oxygen. In such cases, bleaching of TDI might take place through an intermediate species that is still fluorescing, here at around 590 nm (Figure 4d, spectrum 2).

**Single-Molecule Detection on 360-nm Excitation.** We next probed the single-molecule FRET dynamics by optically exciting into the absorption band of NMI and by simultaneously monitoring the fluorescence emitted by the PMI and TDI chromophores. For these experiments we avoided recording the fluorescence spectra to be able to use relatively low excitation powers ( $\sim 0.5$  kW/cm<sup>2</sup>) in order to prevent fast photobleaching.

Within a population of 100 interrogated molecules, individual triad molecules showed either exclusive TDI emission (80%, Figure 5a) or TDI emission followed by activity in both channels (20%, Figure 5c). None of the interrogated triad molecules showed emission solely in the PMI channel. We noticed that, for similar excitation power, the survival time of single triad molecules excited at 360 nm is by far shorter than that of the same molecules excited at 490 nm. Figure 5b shows the probability densities of the survival times for single triad molecules undergoing excitation at 360 nm (upper panel) and 490 nm (lower panel). Exponential fits to the histograms from Figure 5b give time constants of 23 s (360-nm excitation) and 158 s (490-nm excitation). According to the ensemble spectroscopic data reported here, PMI and NMI have quantum yields of fluorescence of 0.98 and of 0.1, respectively. A quantum yield approaching unity reflects a very low efficiency for intersystem crossing (ISC) from the first singlet excited state to the triplet manifold. A previous single-molecule report on a rim-substituted PMI rigid polyphenylenic dendrimer immobilized in Zeonex indicated a rate constant for ISC of around  $6 \times 10^3$  s<sup>-1</sup>, and therefore a quantum yield for ISC of about  $10^{-5}$  s<sup>-1</sup>.<sup>22</sup> For NMI, assuming that nonradiative deactivation is mainly related to triplet formation,<sup>23</sup> for a quantum yield of fluorescence of about 0.1 and a fluorescence lifetime of 0.33 ns, the rate constant and the quantum yield for ISC are estimated to be around  $3 \times 10^{10}$  s<sup>-1</sup> and 0.9, respectively. When NMI is part of the triad and 360-nm excitation is used, NMI fluorescence is quenched from 0.33 ns to 0.04 ns by energy transfer to the TDI core, either directly or in a cascade fashion. Therefore, for a single triad molecule, optical excitation of an NMI chromophore will open competition mainly between triplet formation ( $k_{\text{ISC}} \approx 10^{10}$  s<sup>-1</sup>) and direct energy transfer ( $k_{\text{FRET}} \approx 2.5 \times 10^{10}$  s<sup>-1</sup>). Having such a high quantum yield of triplet formation, the probability of photobleaching of an NMI chromophore on 360-nm excitation becomes considerably higher than the probability of photobleaching of a PMI chromophore on 490-nm excitation. Consequently, the survival time of a single triad molecule becomes substantially shorter on 360-nm excitation than on 490-nm excitation (Figure 5b).

Shown in Figure 5c is an example of a single triad molecule where, on 360-nm laser excitation, bleaching of the TDI is followed by activity in both TDI and PMI channels. For this molecule, bleaching of TDI leads to a drop in the fractional intensity from 1 to 0.5 (Figure 5c), indicating a shift in the fluorescence spectrum toward shorter wavelengths. The lifetimes we detected in the TDI and PMI channels in the region after the bleaching of the TDI are correlated (Figure 5d), suggesting that emission is connected with a single excited species, similar to the intermediate species we identified in the single-molecule experiments at 490-nm laser excitation (Figure 4). On 360-nm excitation, 20% of the interrogated single triad molecules showed such an intermediate species. The fluorescence emitted from the TDI side is the result of excitation energy transfer from the NMI chromophores, either by direct transfer or via stepwise transfer through a PMI. NMI chromophores have a high probability for triplet formation and therefore a high chance to

(21) Christ, T.; Kulzer, K.; Bordat, P.; Basché, T. *Angew. Chem., Int. Ed.* **2001**, *40*, 4192–4195.

(22) Vosch, T.; Cotlet, M.; Hofkens, J.; Van der Biest, K.; Lor, M.; Weston, K.; Tinnefeld, P.; Sauer, M.; Latterini, L.; Müllen, K.; De Schryver, F. C. *J. Phys. Chem. A* **2003**, *107*, 6920–6931.

(23) Wintgens, V.; Valat, P.; Kossanyi, J.; Demeter, A.; Biczok, L.; Berges, T. *New J. Chem.* **1996**, *20*, 1149–1158.



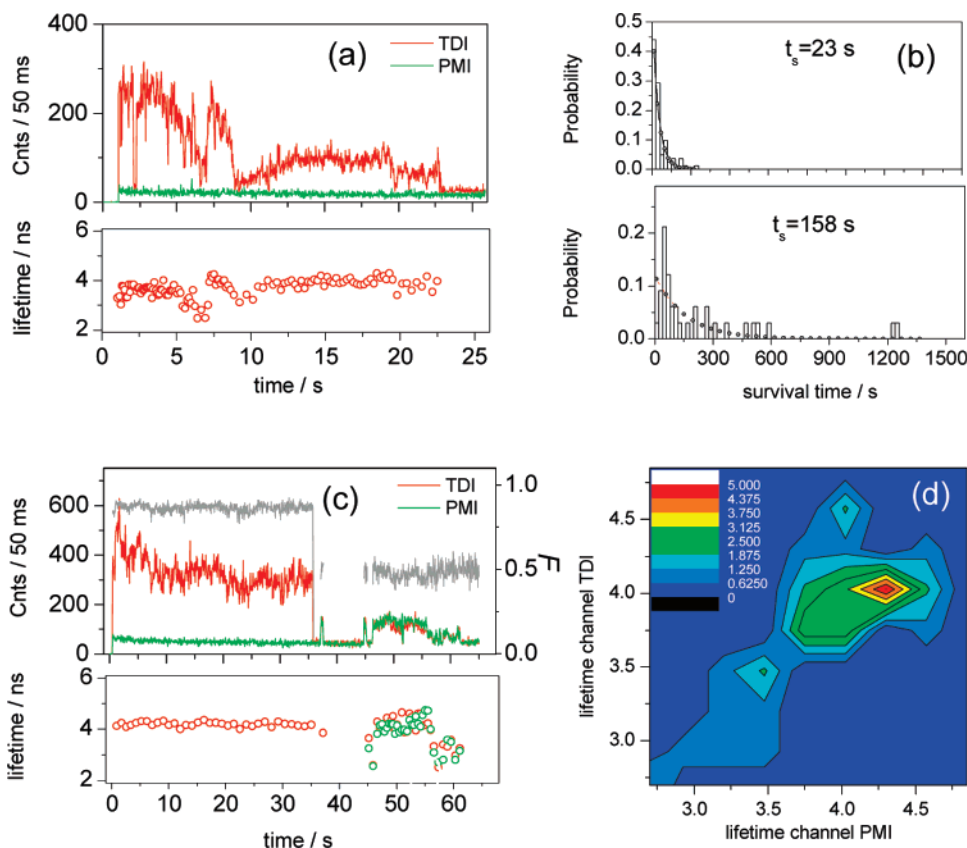


**Figure 5.** Single-molecule results on 360-nm excitation for triad molecules embedded in Zeonex. Properties estimated with photons detected in the TDI channel are colored red, and those estimated with photons detected in the PMI channel are green. (a) Trajectories of the fluorescence intensity (upper panel, red and green lines) and lifetime (lower panel, red circles) from a single triad molecule. (b) Normalized probability densities of the survival time of single triad molecules on 360-nm pulsed excitation (upper panel) and 490-nm pulsed excitation (lower panel). Also shown are exponential fits (line + symbol) to the respective histograms. (c) Trajectories of the fluorescence intensity (upper panel, red and green lines), fractional intensity (upper panel, gray line), and lifetime (lower panel, red and green circles) from another single triad molecule. (d) Contour plot showing the correlation between the single-molecule lifetimes detected in the TDI and PMI channels in the region from 45 to 58 s shown in panel c, upper side.

rapidly photobleach. The higher ISC yield to the triplet state of NMI might lead to the creation of singlet oxygen which can react with the core TDI, leading to the formation of the intermediate species. Consequently, the chance for formation of the intermediate species will be higher if a single triad molecule undergoes excitation at 360 nm than at 490 nm.

As already mentioned, single triad molecules undergoing 360-nm excitation do not show exclusive emission in the PMI channel. According to the triad-related ensemble spectroscopic data and to the molecular-modeling data reported here, upon 360-nm excitation of an NMI chromophore within the triad, the excitation energy can be transferred with almost equal probability either directly or in a cascade fashion to the core TDI. The latter situation involves a PMI chromophore. In view of the interchromophoric distances and Förster radii reported here for different types of pairs of rylene chromophores within the triad, unidirectional FRET from NMI to TDI should take place with an efficiency of 66%, while unidirectional FRET from NMI to PMI, an intermediate acceptor on the way to TDI, should take place with an efficiency of 77%. However, the 360-nm excitation single-molecule data of the triad suggest that PMI chromophores might not be involved in the dynamics of FRET from NMI to TDI. To a certain extent, such a hypothesis is supported by the 360-nm excitation ensemble TCSPC data that show perfect matches between the FRET-related time constants detected in the fluorescence decays monitored at the emission

peaks of NMI (430 nm) and TDI (705 nm). Theoretically, at the single-molecule level and on 360-nm excitation, emission from PMI chromophores might be seen only after the bleaching of the TDI core or of its reduced form, if the latter is formed. With PMI and TDI chromophores with fluorescence quantum yields approaching unity, high photostability, and very inefficient ISC when compared to that of NMI, optical excitation of a single triad molecule at 360 nm will always lead to complete photobleaching of the NMI chromophores before the core TDI might get the chance to photobleach. Therefore, PMI fluorescence will never be observed on such single-molecule experiments.

It is worth mentioning a previous ensemble spectroscopic study on the excitation energy transfer going on in the triad<sup>3</sup> where the authors reported, on the basis of an energetically optimized three-dimensional structure of the molecule computed in HyperChem, center-to-center distances between NMI and PMI and between NMI and TDI as short as 2.15 and 2.75 nm, respectively. For such distances and based on the Förster radii calculated by us, the efficiencies for excitation energy transfer from NMI to PMI and from NMI to TDI will have values of 88% and 42%, respectively. Since such data are sensitive to the mutual orientation of the donor and acceptor chromophores and to the computational methods used to calculate the energetically optimized structure of the triad, it is safe to assume that, within the triad, both excitation energy processes involving

NMI as a donor are possible and in fact will compete with each other.

### Conclusion

We used ensemble and single-molecule fluorescence experiments to investigate competition between directional and cascade energy transfer in a triad system, that is, a polyphenylenic rigid dendrimer bearing a TDI core chromophore, four scaffold-substituted PMI chromophores, and eight rim-substituted NMI chromophores. The spatial positioning of these chromophores within the triad and their respective spectral properties make this multichromophoric system an efficient light collector, able to capture light over the whole visible spectral range and to transfer it, either directly or in a cascade fashion, to the core TDI, where finally it is released as red fluorescence.

Using 490-nm laser excitation, we were able to find evidence for a highly efficient unidirectional FRET from the scaffold-substituted PMIs to the TDI core by means of ensemble TCSPC experiments. Single-molecule experiments on 490-nm excitation evidenced also highly efficient FRET from PMI to TDI, with individual triad molecules emitting fluorescence exclusively from the TDI side in the beginning of their emission. Within the single triad molecules we have interrogated with 490-nm laser light, we have identified the presence of an intermediate form with a single-molecule spectrum similar in shape to that of TDI but with an emission maximum shifted hypsochromically by about  $2000\text{ cm}^{-1}$ . Most probably, the intermediate relates to an oxidized and therefore conjugationally reduced TDI chromophore with spectrally blue-shifted absorption and emission properties relative to those of the non-oxidized TDI.

On 360-nm excitation, NMI chromophores can transfer their excitation energy either directly or in a cascade fashion to the core TDI, the latter case involving a scaffold-substituted PMI chromophore. Within a triad molecule, both processes can be present and will compete with each other. This is because the

emission spectrum of NMI overlaps considerably with both the  $S_0-S_2$  absorption band of TDI and the  $S_0-S_1$  absorption band of PMI and because of the favorable center-to-center distances between NMI donors and PMI as well TDI acceptors in terms of Förster energy transfer. Single-molecule experiments on 360-nm excitation evidence highly efficient FRET from NMI chromophores to the TDI core, with individual triad molecules emitting fluorescence either exclusively from the TDI core or from the intermediate oxidized TDI species. The probability of formation of the oxidized form is higher on 360-nm excitation, most probably because of the creation of singlet oxygen due to the higher intersystem crossing yield to the triplet state of NMIs. However, exclusive PMI fluorescence was not observed for single triad molecules undergoing 360-nm excitation. Whether or not PMI chromophores are involved in the dynamics of FRET from NMI to TDI cannot be sorted out even by the combination of ensemble and single-molecule experiments. PMI and TDI are chromophores with fluorescence quantum yields and high resistance to photobleaching when compared to NMI. Consequently, on 360-nm excitation of a single triad molecule, NMI chromophores might be the first ones to bleach, leaving no chance for PMI to be observed after an eventual bleaching of TDI or of its intermediate form. However, based on the spectral data and the information gained by molecular modeling, energy transfer from rim-substituted NMIs can take place with an almost equal chance to the scaffold-substituted PMIs or to the TDI core.

**Acknowledgment.** Support from FWO, K.U. Leuven (GOA 2001/2), Federal Science Policy of Belgium (IUAP-V-03), and a Max Planck Research Award is acknowledged. Dr. P. M. Goodwin and Dr. J. H. Werner from Los Alamos National Laboratory are thanked for discussions.

JA042656O